Research in Molecular Medicine

A Novel Chimeric Vaccine Targeting Leukemia Inhibitory Factor and Leukemia Inhibitory Factor Receptor: A Computational Approach to Cancer Immunotherapy

Zahra Ghanei[1*], **Fatemeh Sefid**[2]

1. Department of Biotechnology, Faculty of Biological Sciences, Alzahra University, Tehran, Iran.
2. Department of Biology Sciences, School of Materials Engineering and Interdisciplinary Sciences, Shahid Sadoughi University of Medical Sciences, Yazd, Iran.

Use your device to scan and read the article online

Citation Ghanei Z, Sefid F. A Novel Chimeric Vaccine Targeting Leukemia Inhibitory Factor and Leukemia Inhibitory Factor Receptor: A Computational Approach to Cancer Immunotherapy. Research in Molecular Medicine. 2025; 13(3):189-202. https://doi.org/10.32598/rmm.13.3.1453.1

https://doi.org/10.32598/rmm.13.3.1453.1

Article Type:
Research Paper

Article info:
Received: 10 Apr 2025
Revised: 28 Apr 2025
Accepted: 13 Jul 2025

Keywords:
Bioinformatics, Cancer immunotherapy, Chimeric vaccine, Leukemia inhibitory factor (LIF)/LIF receptor®

ABSTRACT

Background: Leukemia inhibitory factor (LIF) and LIF receptor (LIFR) are critical mediators of cellular processes, including immune regulation, stem cell maintenance, and tumor progression. In Oncology, aberrant LIF/LIFR signaling promotes tumor survival and immune evasion. This study presents the computational design of a novel chimeric vaccine targeting immunogenic epitopes derived from human LIF and LIFR.

Materials and Methods: We employed comprehensive in silico methods to investigate the biochemical characteristics, immunogenic epitopes, and potential functional domains of LIF and LIFR. After identifying suitable regions and designing a chimeric vaccine, physicochemical properties and 3D structure were predicted using various bioinformatics tools, both individually and in combination.

Results: The results showed highly antigenic B-cell and T-cell epitopes within LIF (amino acids 70-100) and LIFR (amino acids 700-780), as indicated by a VaxiJen score of 0.9737. A multi-epitope construct was engineered by fusing selected epitopes with flexible GGGGS linkers to enhance immunogenicity and structural stability.

Conclusion: A computationally designed chimeric vaccine targeting LIF and LIFR is a promising cancer immunotherapy strategy. Also, success requires rigorous in vivo validation and optimization, highlighting computational biology's role in cancer treatment innovation and targeting key pathways.

*** Corresponding Author:**
Zahra Ghanei
Address: *Department of Biotechnology, Faculty of Biological Sciences, Alzahra University, Tehran, Iran.*
Phone: *+98 (21) 85692734*
E-mail: *Z.Ghanei@alzahra.ac.ir*

Introduction

Leukemia inhibitory factor (LIF), a pleiotropic cytokine within the interleukin-6 (IL-6) family, mediates critical biological processes (BP) through heterodimerization of its cognate receptor (LIFR) and gp130 co-receptor [1-3]. This signaling complex activates downstream pathways that regulate cellular differentiation and proliferation across diverse tissue types. LIF coordinates pleiotropic signaling of JAK/STAT3, AKT, EKR1/2, and mTOR through ligand-receptor activation [4-6]. LIF first binds to the LIFR subunit, then to gp130, forming a functional complex that can trigger activation of JAK-STAT3, MAPK, AKT, and the mTOR signaling pathway [3, 7].

LIF exhibits multifaceted oncogenic properties through its capacity to drive malignant proliferation across diverse cancer types, including solid tumors, such as colorectal, prostate, and breast cancers [8-11]. The LIF and LIFR partnership constitutes a critical signaling hub governing cancer stem cell (CSC) biology through 3 interconnected dimensions: stemness enforcement, therapy resistance, and metastatic programming [8, 12, 13].

The oncogenic LIF/LIFR signaling pathway has emerged as a critical regulator of CSC maintenance and disease progression. Experimental models demonstrate that genetic silencing of LIF via siRNA in melanoma systems significantly impaired tumor cell proliferation, cellular adhesion, migratory capacity, and colony-forming ability. Parallel studies in pancreatic ductal adenocarcinoma and rhabdomyosarcoma models showed LIFR blockade: Reduced metastatic dissemination in pancreatic carcinoma and rhabdomyosarcoma, diminished CSC properties in ovarian malignancies, and induced apoptosis in breast tumors [4, 14-16]. Active immunotherapy targeting murine LIF/LIFR demonstrated dual efficacy, suppressing CSC-driven tumorigenesis or attenuating established tumor progression compared to control cohorts in a syngeneic mouse model [17]. Two LIF/LIFR-targeted therapeutics—the humanized anti-LIF monoclonal antibody MSC-1 and the first-in-class LIFR inhibitor EC359—are advancing through clinical development [18, 19]. This evidence suggests that the LIF/LIFR axis could be a promising target for cancer immunotherapy [20].

Identifying the antigenic and immunogenic regions of target proteins and designing chimeric vaccines are crucial steps in formulating and advancing novel cancer immunotherapy strategies [21, 22]. Computational vaccine design pipelines that integrate predicted antigen structures reduce preclinical development costs and accelerate lead candidate selection compared with conventional approaches [23, 24].

This study aimed to predict the linear and conformational B-cell epitopes present within the sequences of LIF and LIFR, enabling the identification of the most immunogenic regions for the design of a multivalent vaccine linked by flexible linkers. Targeting these antigens involved in the LIF/LIFR signaling pathways represents a novel strategy with the potential to inhibit signaling associated with stemness, drug resistance, and metastasis. Binding site prediction was employed to identify conserved functional domains in LIF/LIFR, ensuring epitopes disrupt critical protein-protein interactions and enhance vaccine efficacy. At the same time, biological activity analyses linked epitopes to oncogenic signaling pathways, validating their potential to induce therapeutic immune responses.

Materials and Methods

Sequence data availability, BLAST, and conserved domain analysis

The LIF and LIFR protein sequences were obtained from NCBI and saved in FASTA format for further analysis. The LIF and LIFR sequences were used as queries in a BLAST (Basic Local Alignment Search Tool) search against the non-redundant protein database. The same website was used to search for probable conserved domains within the query protein sequences.

PDB search and sequences alignment

The LIF and LIFR protein sequences were used as input for PSI-BLAST searches against the PDB (Protein Data Bank) to identify homologous structures. A protein BLAST search was also performed against the RefSeq Select proteins database using the BLOSUM80 matrix to identify homologous sequences. The RefSeq Select database contains representative NCBI RefSeq protein sequences from human, mouse, and prokaryotes, including one representative protein per protein-coding gene for human and mouse, and RefSeq proteins annotated on reference and representative genomes for prokaryotes. The LIF and LIFR protein sequences with the highest total and maximum BLAST scores were aligned using COBALT (Constraint-based Multiple Alignment Tool) for precise homology analysis. COBALT performs multiple protein sequence alignments using conserved-domain and local-sequence-similarity information.

Signal peptide prediction

The SignalP server was used to predict the presence and location of signal peptide cleavage sites in amino acid sequences from various organisms. This method uses a combination of artificial neural networks to predict both cleavage sites and the presence or absence of a signal peptide.

Homology modelling and structure assessment

SWISS-MODEL, a web-based integrated service, was used for homology modeling of the LIF and LIFR structures. Homology modeling with SWISS-MODEL involves 4 main steps: (i) identification of structural templates, (ii) alignment of the target sequence with the template structure(s), (iii) model building, and (iv) model quality evaluation. These steps require specialized software and integrate up-to-date protein sequence and structure databases. The process can be iterative, repeating these steps until a satisfactory modeling result is achieved. The structure assessment service within SWISS-MODEL integrates various tools and annotations with sequence and structure viewers to simplify the exploration of quality and structural features of macromolecular models. Assessment can be performed independently or in comparison to a reference structure.

Biological function annotation

COFACTOR is a method for annotating the biological function of proteins. It uses a combination of structural, sequence, and protein-protein interaction (PPI) data. Given a 3D protein structure, COFACTOR searches the BioLiP database to identify functional sites and homologs. This process allows COFACTOR to infer functional information, including gene ontology (GO) terms, enzyme commission (EC) numbers, and ligand-binding sites. GO term predictions are further refined using sequence and profile alignments from UniProt-GOA, and PPI data from STRING.

Pockets, interfaces, and ligand binding site prediction

Mathematical morphology is employed by GHECOM (Grid-based HECOMi Finder) to identify pockets on protein surfaces, regardless of their size.

We used InterProSurf, which predicts functional sites on protein surfaces using patch analysis.

Ligand binding site predictions for LIF and LIFR were performed using the eF-seek web server. Since a protein's three-dimensional structure dictates its function, structural similarities can indicate functional relationships. Interactions with ligands are frequently the first step in molecular function (MF). Given a PDB file, eF-seek employs a proprietary algorithm, based on clique detection, to search the eF-site database for comparable binding sites.

Single-scale amino acid properties assay

The BcePred server with 58.7% accuracy was used to predict potential antigenic regions in LIF and LIFR sequences. BcePred uses individual or combined physicochemical properties (hydrophilicity, flexibility, mobility, accessibility, polarity, exposed surface, and turns) to identify B-cell epitopes. The Immune Epitope Database (IEDB) server similarly uses properties like hydrophilicity, flexibility, accessibility, turns, and antigenic propensity, reflecting a broader effort to predict B-cell epitopes from protein sequence characteristics.

Epitope mapping

Several tools were used to predict B-cell epitopes. BepiPred identifies linear epitopes using a hidden Markov model and propensity scale method. SVMTriP predicts antigenic epitopes using a support vector machine (SVM) that combines tri-peptide similarity and propensity scores, validated with a leave-one-out test. ElliPro predicts both linear and discontinuous antibody epitopes. DiscoTope focuses on discontinuous B-cell epitopes, using surface accessibility calculations and a novel epitope propensity score that combines spatial proximity and contact numbers. T cell epitopes were also computed using the MHC I and MHC II binding peptide prediction tools available at IEDB. T cell epitopes were predicted using the IEDB-recommended method, and an HLA allele reference set was selected; epitopes with percentile rank <2 were selected. A rank of ≤2% is often considered a strong binder, while ranks >10% are considered weak or non-binders.

Immunogenic regions selection

Vaccine candidates were selected based on regions with high concentrations of both linear and conformational epitopes, further qualified by single-scale amino acid property assays. Region selection also considered factors like predicted antigenicity probability, average physicochemical properties, and isoelectric point (pI). Two regions were selected as promising antigenic can-

didates, and further analyses were conducted to validate the selection. These analyses included predicting antigenicity probability using VaxiJen, calculating average physicochemical properties via the IEDB server, and determining properties like molecular weight, theoretical pI, amino acid composition, charge, instability index, and aliphatic index using ProtParam. These analyses were also performed on the full LIF and LIFR sequences for comparison with the selected regions.

Final conjugate vaccine design

A flexible linker (GGGGS) was used to connect the selected regions. This linker was chosen to enhance the folding and stability of the fusion proteins, promoting correct orientation and minimizing interference with the folding of individual protein domains. The Phyre2 server predicted the 3D structures of both the selected regions and the conjugate vaccine.

Results

Sequence data, BLAST searching, and conserved domain analysis

Protein sequences for LIF and LIFR, with accession numbers NP_002300.1 and NP_001351226.1, respectively, were retrieved from the NCBI RefSeq database.

A BLAST search matched the query sequences to many others, some from species besides homo sapience. Analysis identified several likely conserved domains within these sequences. The LIF sequence (residues 34-191) primarily aligns with the LIF and Oncostatin M (OSM) superfamily. Within the LIFR sequence, a LIF receptor D2 domain and three fibronectin type III domains were found. Fibronectin type III domains are repeating units within the fibronectin protein. The tenth of these repeats features an RGD sequence, a crucial cell-recognition motif, located in a flexible region. This domain type is common, occurring in about 2% of animal proteins, including various cell-surface receptors and adhesion molecules, as well as some bacterial enzymes.

The D2 domain resides in cytokine-binding module 1 (CBM1) of LIFR and OSMR. The extracellular portion of LIFR is modular, containing two CBMs, an Ig-like domain, and three Fibronectin Type III domains near the cell membrane. The D2 domain in CBM1 resembles those in gp130 and IL-6R alpha, sharing key structural elements, such as the WSXWS motif, which acts as a switch for receptor activation.

PDB search and sequence alignments

A BLAST search of the PDB returned several hits. The highest-scoring result, chosen as the template, included LIF (Chain C, 7N0A_C, Homo sapiens LIF, 100% identity, 89% query coverage) and LIFR (Chain B, 8D6A_B, Homo sapiens LIFR, 99.37% identity, 72% query coverage).

To analyze homology, 10 LIFR and 3 LIF protein sequences were selected from the RefSeq database based on their highest total and maximum scores. Multiple sequence alignment was performed using COBALT, a progressive alignment tool. COBALT leverages pairwise constraints from conserved-domain databases (via RPS-BLAST), protein motif databases (via BLASTP), and local sequence similarity (via PHI-BLAST). COBALT accelerates computation by clustering sequences with numerous shared words, then identifying conserved domains and motifs for only one representative sequence per cluster. Figure 1 illustrates the alignment results, using a color scheme to represent conservation. This scheme, based on relative entropy, highlights amino acid conservation: red for high conservation and blue for low conservation. Only gap-free positions are colored.

Signal peptide prediction, homology modeling, and structural assessment

SignalP server predicts a cleavage site between positions 44 and 45 (probability: 0.5110) in LIFR and between positions 22 and 23 (probability: 0.8823) in LIF, based on a combination of several artificial neural networks.

SWISS-MODEL generated four models for LIFR and two for LIF. The best model for each was selected for further analysis. The optimal LIFR model exhibited a GMQE (Global Model Quality Estimate) of 0.58 and a QMEANDisCo Global score of 0.76±0.05. For LIF, the best model had a GMQE of 0.74 and a QMEANDisCo Global score of 0.76±0.06 (Figure 2).

GMQE combines properties of the target-template alignment and template structure to estimate model quality. The QMEANDisCo Global score represents the average per-residue score from the QMEANDisCo scoring function, a composite score for single-model quality estimation. QMEANDisCo incorporates single-model scores and a consensus component, leveraging information from homologous, experimentally determined protein structures. Figure 2, the "local quality" plot, displays the expected similarity to the native structure (y-axis) for

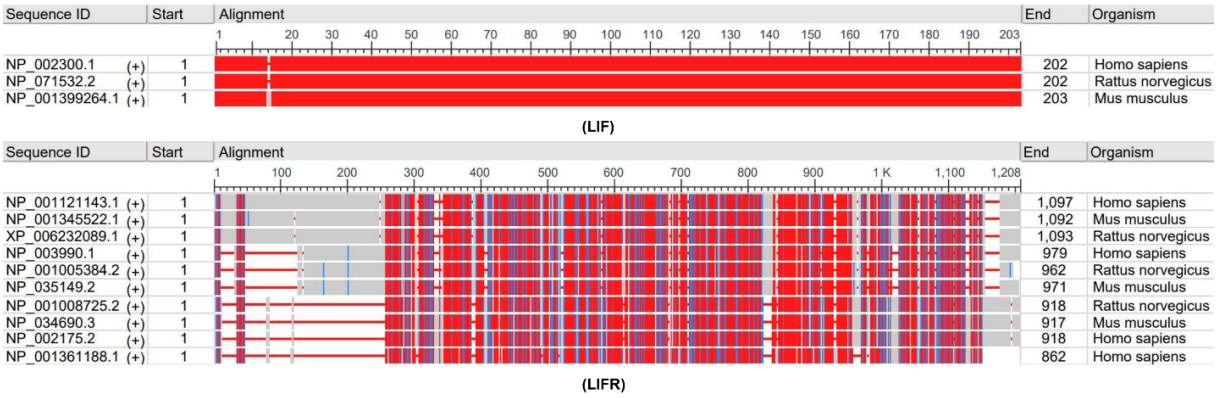

Figure 1. Illustration of alignment results with conservation color scheme in LIF (top) and LIFR (bottom)

each residue in the model (x-axis). Residues with scores below 0.6 are generally considered low quality. Figure 3 presents the Ramachandran plots of the predicted models. A Ramachandran plot visualizes energetically favorable regions for backbone dihedral angles (ψ against φ) of amino acid residues in a protein structure.

Biological function annotation

COFACTOR analysis revealed ligand binding sites involving conserved residues in both LIF and LIFR (Figure 4). Specifically, residues 41, 47, 50, 51, 54, 142, 146, 149, and 150 of LIF exhibited a high binding site similarity score (BS-score=1.88), as did residues 445, 446, 447, and 497 of LIFR (BS-score=1.73). A BS-score above 1 suggests a significant local match between the predicted and template binding sites. Predicted GO terms for these proteins, categorized by MF, BP, and cellular component (CC), are detailed in Table 1.

Detection of pockets, interfaces, and ligand binding sites

GHECOM utilizes mathematical morphology to identify 5 pockets on the surfaces of LIF and LIFR. For each residue, GHECOM calculates a "pockets score" using the formula:

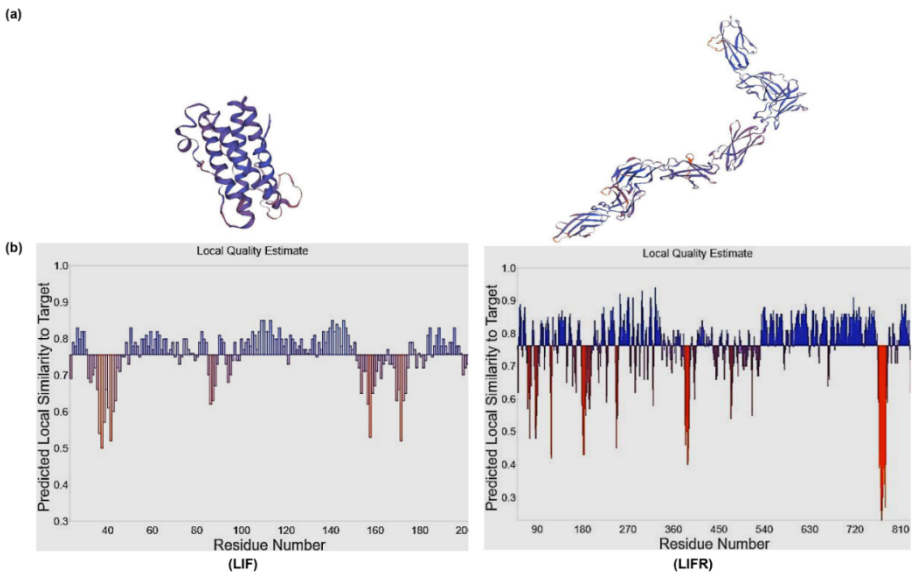

Figure 2. SWISS-MODEL predictions

a) LIF (left) and LIFR (right) 3D structure based on confidence color scheme (residues are colored by their local quality value), b) The "local quality" plot for each model residue (x-axis) shows the expected similarity to the native structure (y-axis)

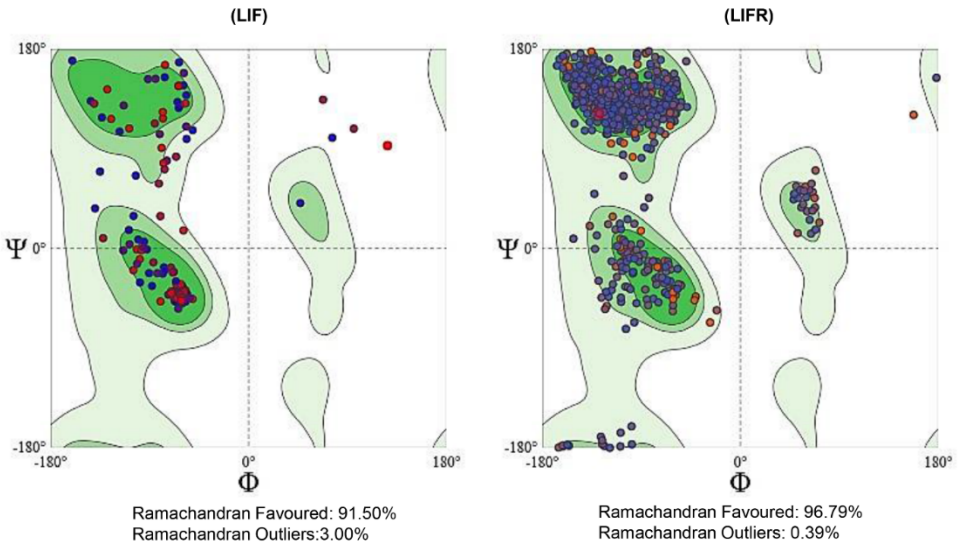

Figure 3. Ramachandran plot of predicted models for LIF (left) and LIFR (right)

This score reflects pocket depth and size; deeper, larger pockets yield higher values. Results indicate that pockets associated with small-molecule binding sites and active sites exhibit scores above the average, with active sites demonstrating significantly higher values. These findings suggest that pocket analysis can aid in predicting binding and active sites from protein structures. A three-dimensional visualization of GHECOM-predicted pockets, colored by "pocketness," is presented in Figure 5.

InterProScan analysis reveals functional sites on the protein's surface. Specifically, residues 107, 166, 167, 168, 169, 28, 30, 114, 117, and 118 are identified as the most significant functional sites in the LIF protein, while residues 146, 148, 151, 207, 209, 210, 211, 212, 214, 244, 246, 432, and 517 are highlighted in the LIFR structure. These predicted functional residues on the protein structures' surfaces, as determined by InterProSurf, are visualized in Figure 6.

eF-seek analysis predicts potential binding sites (PBS) on protein surfaces by identifying residues or atoms near known ligand-binding regions. For LIFR, the predicted PBS with the highest score (0.76888) is located at residues C:573, 581-587, 593-597. The predicted PBS for LIF with the highest score (0.60694) are located at B:85-95, 190, 193, 194, 197, 200. These predictions are visualized in Figure 7.

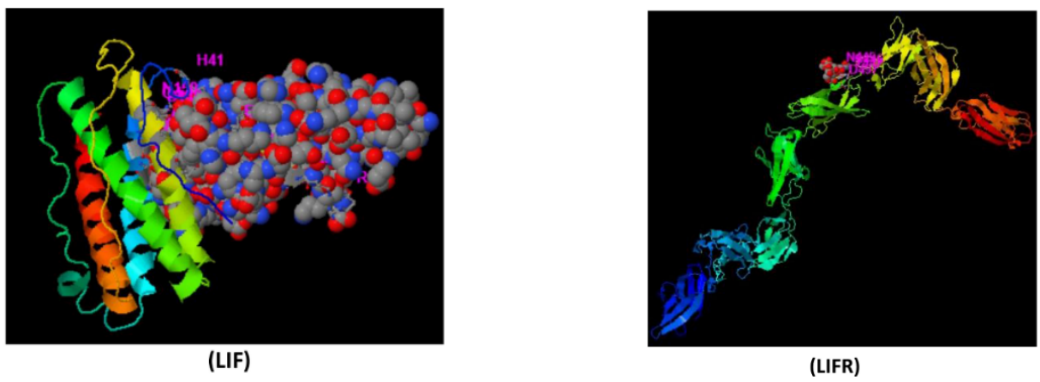

Figure 4. Ligand binding sites determined using COFACTOR for LIF (left) and LIFR (right)

Table 1. Predicted GO terms including MF, BP, and CC

Variables		Leukemia Inhibitory Factor	Leukemia Inhibitory Factor Receptor
MF	GO term	GO:0005146	GO:0004872
	CscoreGO	1.00	0.74
	Name	Leukemia inhibitory factor receptor binding	Receptor activity
BP	GO term	GO:2000026	GO:0065007
	CscoreGO	1.00	0.90
	Name	Regulation of multicellular organismal development	Biological regulation
CC	GO term	GO:0044464	GO:0044464
	CscoreGO	0.87	0.91
	Name	Cell part	Cell part

Single-scale amino acid properties assay

IEDB and BcePred analyses predict several properties of the protein sequence, including hydrophilicity, accessibility, antigenicity, flexibility, and beta-turn secondary structure. While single-scale amino acid properties were detectable across the entire sequence length, the most prominent regions with higher probability were located at positions 60–100 in LIF and 690-788 in LIFR.

Epitope mapping

Linear B-cell epitope prediction reveals distinct patterns in LIF and LIFR. BepiPred analysis indicates a concentration of LIFR epitopes within the 700-744 region, while LIF epitopes are more prominent in the 18-43 region. A high density of linear epitopes is also observed in LIF between positions 70 and 101. SVMtrip identified 10 linear B-cell epitopes in LIF and 2 in LIFR, based on their respective scores. The top-ranked epitopes were "ANGTEKAKLVELYRIVVYLG" (LIF, positions 94–113) and "GYQLLRSMIGYIEELAPIVA" (LIFR, positions 708–727). ElliPro predicted

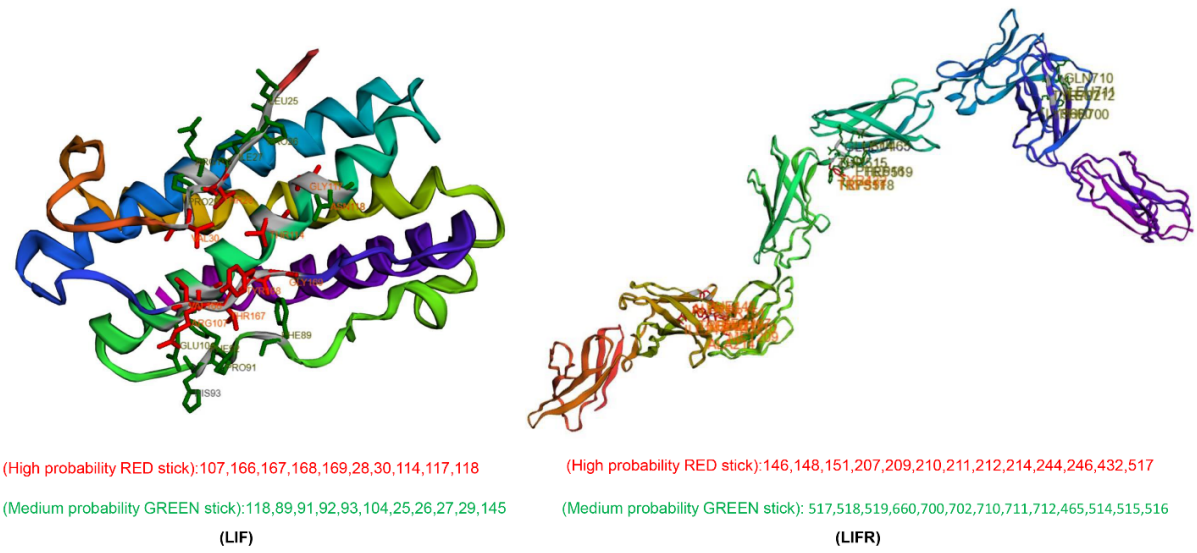

Figure 5. 3D Leukemia inhibitory factoriew of pockets predicted by the GHECOM server based on pocketness color in LIF (left) and LIFR (right)

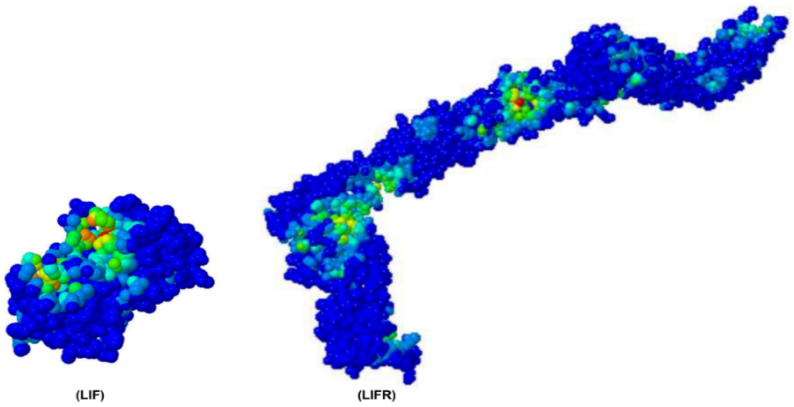

Figure 6. Interprosurf protein-protein interaction prediction and residues predicted by auto patch analysis in LIF (left) and LIFR (right)

7 linear and 4 discontinuous B-cell epitopes for LIF, and 17 linear and seven discontinuous epitopes for LIFR. The highest-ranked linear epitopes were "DTSGKDVFQ" (LIF, positions 171-179) and the longer sequence "FLRGYLFY-FGKGERDTSKMRVLESGRSDIKVKNITDISQKTLRI-ADLQGKTSYHLVLRAYTDGGVGPEKSMYVVTKE" (LIFR, positions 755-831). Figure 8 illustrates the best discontinuous and linear epitopes, highlighting their protrusion index (PI). DiscoTope predicted discontinuous B-cell epitopes, including residues 172-176 in LIF and a more extensive set of residues in LIFR: 162, 167, 193, 195-198, 473-476, 536, 560-565, 567, 590, 629, and 768-774.

T-cell epitopes were predicted using MHC binding tools available in the immune epitope database (IEDB). The MHC I binding server identified a significant number of epitopes in both LIF and LIFR proteins. Similarly, MHC II binding analysis predicted numerous epitopes in both proteins. The results, summarized in Table 2, highlight a subset of peptides with percentile ranks <1, indicating strong binding affinity.

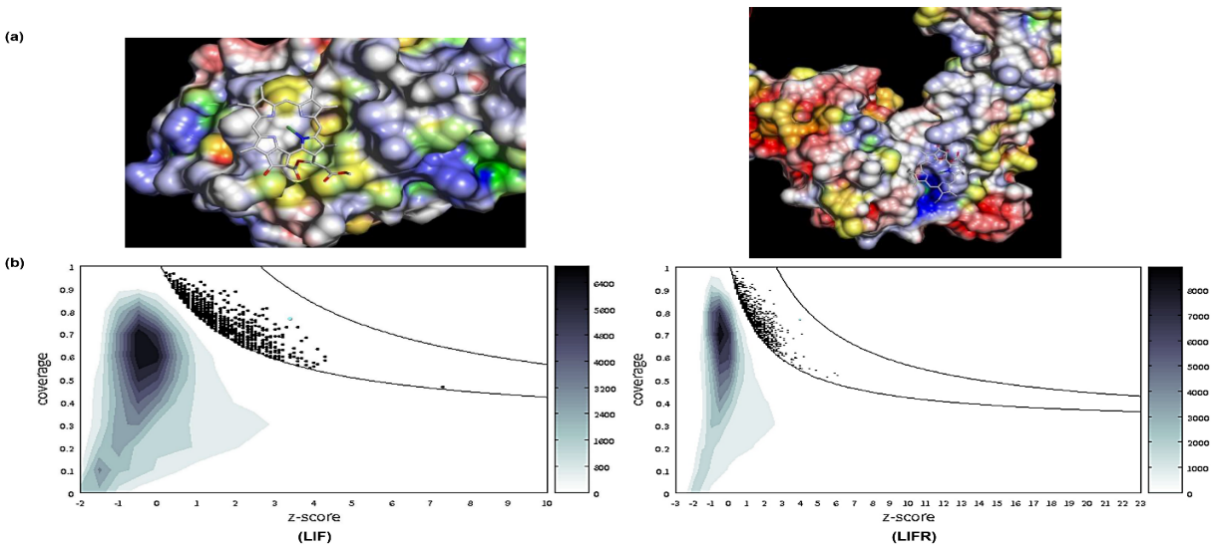

Figure 7. eF-seek predictions

a) The complex structure of the results is shown for LIF (left) and LIFR (right), b) The density plots are illustrated above.

Note: Dots in the upper right regions indicate "significantly" similar binding sites, and the lower left region indicates the non-similar binding sites. The points above the line in the density plot indicate the "significant" match, with the higher score highlighted in blue.

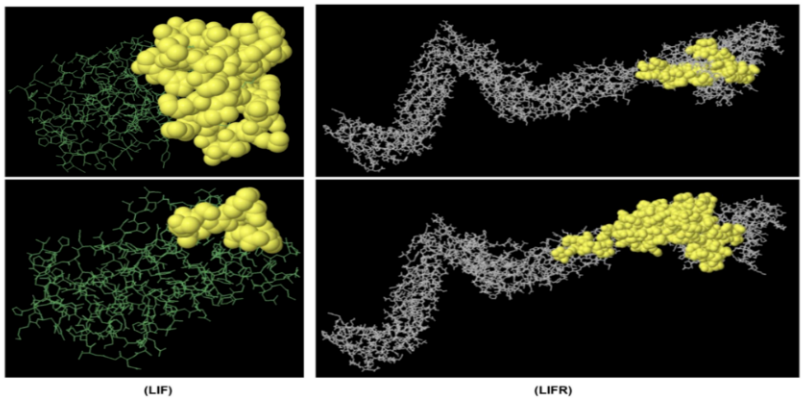

Figure 8. Linear (upper) and discontinuous (lower) epitopes with the highest PI in LIF (left) and LIFR (right)

Immunogenic regions selection

Regions exhibiting dense clusters of both linear and conformational epitopes represent potential vaccine candidates. These regions require further characterization using single-scale amino acid property analysis.

Based on epitope mapping, two regions were selected as vaccine candidates: Residues 70-100 of LIF and 700-780 of LIFR. Several properties of these candidates were compared to their respective parent proteins, including VaxiJen antigenicity score, protrusion index (PI), instability index, solubility, hydrophilicity, accessibility, flexibility, and secondary structure. Table 3 summarizes the average physicochemical properties of the selected regions (calculated using the IEDB server), along with ProtParam-derived properties, including molecular weight and theoretical PI, for both candidates and their parent proteins.

Further Scrutiny

A flexible (GGGGS)3 linker was employed to connect 2 regions of our vaccine candidates (Figure 9), as this linker has demonstrated improved folding and stability in fusion proteins. The resulting chimeric vaccine achieved a VaxiJen score of 0.9737, surpassing the scores of the individual regions. Key characteristics of the final vaccine, such as the VaxiJen score, physicochemical properties, amino acid count, and molecular weight, are detailed in Table 2. The conservation profiles of the predicted epitopes were analyzed, confirming their specificity for LIF/LIFR and minimal conservation across unrelated human proteins, thereby ensuring vaccine safety.

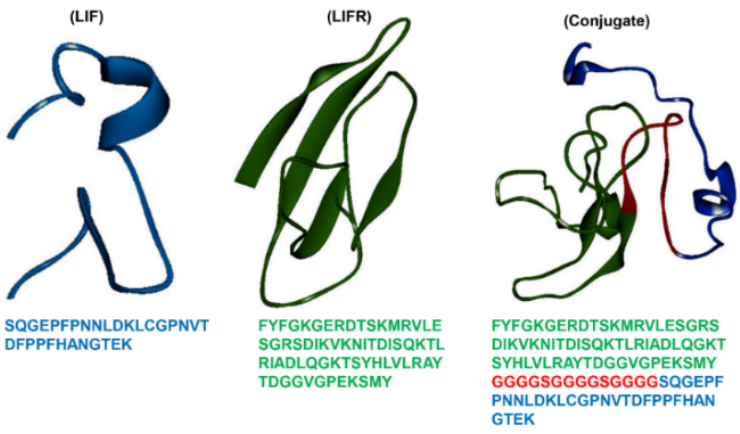

Figure 9. 3D structure and sequences of LIF and LIFR and conjugate vaccine candidates

Table 2. Prediction of T cell epitopes by the IEDB server

MHC I/II Binding Peptide	Protein	Allele	Position	Peptide	Percentile Rank
MHC I binding epitopes	LIF	HLA-B*08:01	75-83	TEKAKLVEL	0.538494
		HLA-A*01:01	36-44	SANALFILY	0.558077
		HLA-B*44:03	81-89	VELYRIVVY	0.744457
		HLA-A*03:01	735-743	TSADSILVK	0.613162
	LIFR	HLA-A*02:01	126-134	TLNEQNVSL	0.940818
		HLA-A*02:01	714-722	SMIGYIEEL	0.964418
MHC I binding epitopes	LIF	HLA-DRB3*02:02	87-101	TDFPPFHANGTEKAK	0.04
		HLA-DRB1*03:01	115-129	SLGNITRDQKILNPS	0.07
		HLA-DRB1*15:01	83-97	GPNVTDFPPFHANGT	0.52
		HLA-DRB3*01:01	864-878	WIKETFYPDIPNPEN	0.16
	LIFR	HLA-DRB3*01:01	591-605	QHKAEIRLDKNDYII	0.16
		HLA-DRB3*01:01	866-880	KETFYPDIPNPENCK	0.17

Discussion

Aberrant LIF/LIFR signaling is a hallmark of aggressive malignancies, driving tumor stemness, metastasis, and therapy resistance [25-27]. The development of a chimeric vaccine targeting LIF/LIFR represents a novel immunotherapeutic strategy to counteract tumor survival and immune evasion mechanisms driven by aberrant LIF/LIFR signaling. This study leverages advanced computational methodologies to design a structurally stable and immunogenic multi-epitope construct. The study's strength lies in its multifaceted computational

Table 3. Physicochemical properties of the average of the selected regions compared to their parent protein

Variables	Conjugate Vaccine	LIF		LIFR	
		Full Length	Vaccine Candidate	Full Length	Vaccine Candidate
VaxiJen score	0.9737	0.4348	0.5536	0.6330	0.8593
Hydrophilicity	2.797	0.768	1.713	1.432	2.416
Antigenicity	1.091	1.061	1.018	1.027	1.042
Flexibility	1.041	0.986	1.018	1.002	1.025
Accessibility	1.000	1.000	1.000	1.000	1.000
Beta-Turn	1.123	0.990	1.152	1.006	1.013
Linear epitope 2.0	0.559	0.481	0.485	0.511	0.541
Linear epitope 1.0	0.759	0.236	0.962	0.061	0.258
Molecular weight	11669.96	22007.74	3156.43	88604.49	7457.51
Theoretical PI	8.75	9.44	4.31	6.22	9.57

approach to vaccine design. The utilization of homology modeling, fold recognition, and ab initio methods to determine the 3D structure of the chimeric vaccine construct is crucial. Accurate structural prediction is essential for understanding the protein's biochemical properties, identifying potential immunogenic epitopes, and predicting its interaction with the immune system [28-31]. The integration of bioinformatics pipelines for characterizing biochemical properties and functional domains further strengthens the analysis.

Epitope density is known to correlate directly with antigenicity and immunogenicity. The inclusion of B cell and T cell epitopes ensures a comprehensive immune activation, which is crucial for targeting tumors that often employ multiple mechanisms to evade immune detection [32, 33]. While discontinuous B cell epitopes are more common, experimental studies often prioritize the identification of linear B cell epitopes. This approach is further justified by the established relationship between epitope density and epitope-specific humoral immune responses [34, 35]. The identification of B cell and T cell epitopes within LIF (amino acids 70-100) and LIFR (amino acids 700-780) with high antigenicity and a VaxiJen score of 0.9737 is a significant finding. This score, combined with the multi-epitope construct, suggests that the vaccine could effectively stimulate both humoral and cellular immune responses [36]. The selection of these epitopes reflects a rational strategy to target key regions of LIF/LIFR involved in oncogenic signaling. Flexible linkers in fusion proteins enhance synthesis efficiency, biological activity, overexpression yield, and pharmacokinetic profiles. By integrating active site prediction and biological activity analyses, this study bridges epitope prediction with therapeutic outcomes, aligning with advancements in neoantigen vaccine design targeting driver mutations. The structural flexibility of these linkers, often composed of small, hydrophilic amino acids like glycine and serine, facilitates inter-domain interactions and movements [37-39]. The engineering of a multi-epitope construct using flexible GGGGS linkers is a common and effective strategy in vaccine design. GGGGS linkers are known to enhance immunogenicity and structural stability by facilitating proper folding and presentation of epitopes to the immune system [40, 41]. This design element is crucial for maximizing the vaccine's potential to elicit a robust and targeted immune response. While the computational design is promising, it is essential to acknowledge the limitations of in silico studies. The vaccine's predicted efficacy needs to be validated through in vitro and in vivo experiments. Further research should focus on evaluating the vaccine's ability to induce a strong and durable anti-tumor immune response in preclinical models. The assessment of potential off-target effects and the optimization of the vaccine delivery system are also critical steps in translating this computational design into a viable cancer immunotherapy.

Conclusion

The computational design of a chimeric vaccine targeting LIF and LIFR represents a significant advancement in cancer immunotherapy. By disrupting oncogenic signaling and eliciting tumor-specific immunity, this vaccine holds promise as a novel therapeutic strategy. However, its success will depend on rigorous in vivo validation and further optimization. This study exemplifies the potential of computational biology to drive innovation in cancer treatment and underscores the importance of targeting key molecular pathways in oncology.

Ethical Considerations

Compliance with ethical guidelines

There were no ethical considerations to be considered in this research.

Funding

This research did not receive any grant from funding agencies in the public, commercial, or non-profit sectors.

Authors contribution's

Conceptualization and investigation: All authors; Methodology: Fateme Sefid; Writing the original draft: Fateme Sefid; Review, and editing: Zahra Ghanei.

Conflict of interest

The authors declared no conflict of interest.

Acknowledgements

The authors would like to thank the staff of Alzahra University and Shahid Sadoughi University of Medical Sciences.

References

[1] Boulanger MJ, Bankovich AJ, Kortemme T, Baker D, Garcia KC. Convergent mechanisms for recognition of divergent cytokines by the shared signaling receptor gp130. Mol Cell. 2003; 12(3):577-89. [DOI:10.1016/S1097-2765(03)00365-4] [PMID]

[2] Cheng JG, Chen JR, Hernandez L, Alvord WG, Stewart CL. Dual control of LIF expression and LIF receptor function regulate Stat3 activation at the onset of uterine receptivity and embryo implantation. Proceed Natl Acad Sci. 2001; 98(15):8680-5. [DOI:10.1073/pnas.151180898] [PMID]

[3] Nicola NA, Babon JJ. Leukemia inhibitory factor (LIF). Cytokine & growth factor reviews. 2015; 26(5):533-44. [DOI:10.1016/j.cytogfr.2015.07.001] [PMID]

[4] Li X, Yang Q, Yu H, Wu L, Zhao Y, Zhang C, et al. LIF promotes tumorigenesis and metastasis of breast cancer through the AKT-mTOR pathway. Oncotarget. 2014; 5(3):788. [DOI:10.18632/oncotarget.1772] [PMID]

[5] Cherepkova MY, Sineva GS, Pospelov VA. Leukemia inhibitory factor (LIF) withdrawal activates mTOR signaling pathway in mouse embryonic stem cells through the MEK/ERK/TSC2 pathway. Cell Death Dis. 2016; 7(1):e2050-e. [DOI:10.1038/cddis.2015.387] [PMID]

[6] Yue X, Wu L, Hu W. The regulation of leukemia inhibitory factor. Cancer Cell Microenviron. 2015; 2(3):e877. [PMID]

[7] Rassouli H, Nemati S, Rezaeiani S, Sayadmanesh A, Gharaati MR, Salekdeh GH, et al. Cloning, expression, and functional characterization of in-house prepared human leukemia inhibitory factor. Cell J. 2013; 15(2):190.

[8] Liu SC, Tsang NM, Chiang WC, Chang KP, Hsueh C, Liang Y, et al. Leukemia inhibitory factor promotes nasopharyngeal carcinoma progression and radioresistance. J Clin Invest. 2013; 123(12):5269-83. [DOI:10.1172/JCI63428] [PMID]

[9] Yu H, Yue X, Zhao Y, Li X, Wu L, Zhang C, et al. LIF negatively regulates tumour-suppressor p53 through Stat3/ID1/MDM2 in colorectal cancers. Nat Commun. 2014; 5(1):5218. [DOI:10.1038/ncomms6218] [PMID]

[10] Wysoczynski M, Miekus K, Jankowski K, Wanzeck J, Bertolone S, Janowska-Wieczorek A, et al. Leukemia inhibitory factor: a newly identified metastatic factor in rhabdomyosarcomas. Cancer Res. 2007; 67(5):2131-40. [DOI:10.1158/0008-5472.CAN-06-1021] [PMID]

[11] Dhingra K, Sahin A, Emami K, Hortobagyi GN, Estrov Z. Expression of leukemia inhibitory factor and its receptor in breast cancer: A potential autocrine and paracrine growth regulatory mechanism. Breast Cancer Res Treat. 1998; 48:165-74. [DOI:10.1023/A:1005942923757] [PMID]

[12] McLean K, Tan L, Bolland DE, Coffman LG, Peterson LF, Talpaz M, et al. Leukemia inhibitory factor functions in parallel with interleukin-6 to promote ovarian cancer growth. Oncogene. 2019; 38(9):1576-84. [DOI:10.1038/s41388-018-0523-6] [PMID]

[13] Christianson J, Oxford JT, Jorcyk CL. Emerging perspectives on leukemia inhibitory factor and its receptor in cancer. Front Oncol. 2021; 11:693724. [DOI:10.3389/fonc.2021.693724] [PMID]

[14] Randolph L, Joshi J, Rodriguez Sanchez AL, Pratap UP, Gopalam R, Chen Y, et al. Significance of LIF/LIFR Signaling in the progression of obesity-driven triple-negative breast cancer. Cancers. 2024; 16(21):3630. [DOI:10.3390/cancers16213630] [PMID]

[15] Wu Y, Xu M, Feng Z, Wu H, Wu J, Ha X, et al. AUF1-induced circular RNA hsa_circ_0010467 promotes platinum resistance of ovarian cancer through miR-637/LIF/STAT3 axis. Cell Mol Life Sci. 2023; 80(9):256. [DOI:10.1007/s00018-023-04906-5] [PMID]

[16] Wang J, Karime C, Majeed U, Starr JS, Borad MJ, Babiker HM. Targeting leukemia inhibitory factor in pancreatic adenocarcinoma. Exp Opin Invest Drug. 2023; 32(5):387-99. [DOI:10.1080/13543784.2023.2206558] [PMID]

[17] Ghanei Z, Mehri N, Jamshidizad A, Joupari MD, Shamsara M. Immunization against leukemia inhibitory factor and its receptor suppresses tumor formation of breast cancer initiating cells in BALB/c mouse. Sci Rep. 2020; 10(1):11465. [DOI:10.1038/s41598-020-68158-0] [PMID]

[18] Shahraz A, Penney M, Candido J, Opoku□Ansah G, Neubauer M, Eyles J, et al. A mechanistic PK/PD model of AZD0171 (anti□LIF) to support Phase II dose selection. CPT. 2024; 13(10):1670-81. [DOI:10.1002/psp4.13204] [PMID]

[19] Viswanadhapalli S, Luo Y, Sareddy GR, Santhamma B, Zhou M, Li M, et al. EC359: A first-in-class small-molecule inhibitor for targeting oncogenic LIFR signaling in triple-negative breast cancer. Mol Cancer Ther. 2019; 18(8):1341-54. [DOI:10.1158/1535-7163.MCT-18-1258] [PMID]

[20] Viswanadhapalli S, Dileep KV, Zhang KY, Nair HB, Vadlamudi RK. Targeting LIF/LIFR signaling in cancer. Gene Dis. 2022; 9(4):973-80. [DOI:10.1016/j.gendis.2021.04.003] [PMID]

[21] Floudas C, Fung H, McAllister S, Mönnigmann M, Rajgaria R. Advances in protein structure prediction and de novo protein design: A review. Chem Engin Sci. 2006; 61(3):966-88. [DOI:10.1016/j.ces.2005.04.009]

[22] Khalili S, Rahbar MR, Dezfulian MH, Jahangiri A. In silico analyses of Wilms' tumor protein to designing a novel multi-epitope DNA vaccine against cancer. J Theor Biol. 2015; 379:66-78. [DOI:10.1016/j.jtbi.2015.04.026] [PMID]

[23] Haste Andersen P, Nielsen M, Lund O. Prediction of residues in discontinuous B□cell epitopes using protein 3D structures. Protein Sci. 2006; 15(11):2558-67. [DOI:10.1110/ps.062405906] [PMID]

[24] Khalili S, Jahangiri A, Borna H, Ahmadi Zanoos K, Amani J. Computational vaccinology and epitope vaccine design by immunoinformatics. Acta Microbiol Immun Hung. 2014; 61(3):285-307. [DOI:10.1556/amicr.61.2014.3.4] [PMID]

[25] Tang W, Ramasamy K, Pillai SM, Santhamma B, Konda S, Pitta Venkata P, et al. LIF/LIFR oncogenic signaling is a novel therapeutic target in endometrial cancer. Cell Death Discov. 2021; 7(1):216. [DOI:10.1038/s41420-021-00603-z] [PMID]

[26] Zhang C, Liu J, Wang J, Hu W, Feng Z. The emerging role of leukemia inhibitory factor in cancer and therapy. Pharmacol Ther. 2021; 221:107754. [DOI:10.1016/j.pharmthera.2020.107754] [PMID]

[27] Liu B, Lu Y, Li J, Liu Y, Liu J, Wang W. Leukemia inhibitory factor promotes tumor growth and metastasis in human osteosarcoma via activating STAT 3. Apmis. 2015; 123(10):837-46. [DOI:10.1111/apm.12427] [PMID]

[28] Baker D, Sali A. Protein structure prediction and structural genomics. Science. 2001; 294(5540):93-6. [DOI:10.1126/science.1065659] [PMID]

[29] Whisstock JC, Lesk AM. Prediction of protein function from protein sequence and structure. Rev Biophys. 2003; 36(3):307-40. [DOI:10.1017/S0033583503003901] [PMID]

[30] Delany I, Rappuoli R, De Gregorio E. Vaccines for the 21st century. EMBO Mol Med. 2014; 6(6):708-20. [DOI:10.1002/emmm.201403876] [PMID]

[31] Zhang Y. Progress and challenges in protein structure prediction. Curr Opin Struct Biol. 2008; 18(3):342-8. [DOI:10.1016/j.sbi.2008.02.004] [PMID]

[32] Purcell AW, McCluskey J, Rossjohn J. More than one reason to rethink the use of peptides in vaccine design. Nat Rev Drug Discov. 2007; 6(5):404-14. [DOI:10.1038/nrd2224] [PMID]

[33] Parvizpour S, Pourseif MM, Razmara J, Rafi MA, Omidi Y. Epitope-based vaccine design: A comprehensive overview of bioinformatics approaches. Drug Discov Today. 2020; 25(6):1034-42. [DOI:10.1016/j.drudis.2020.03.006] [PMID]

[34] Chen J, Liu H, Yang J, Chou KC. Prediction of linear B-cell epitopes using amino acid pair antigenicity scale. Amino Acids. 2007; 33:423-8. [DOI:10.1007/s00726-006-0485-9] [PMID]

[35] Liu W, Chen YH. High epitope density in a single protein molecule significantly enhances antigenicity as well as immunogenicity: A novel strategy for modern vaccine development and a preliminary investigation about B cell discrimination of monomeric proteins. Eur J Immun. 2005; 35(2):505-14. [DOI:10.1002/eji.200425749] [PMID]

[36] Doytchinova IA, Flower DR. VaxiJen: A server for prediction of protective antigens, tumour antigens and subunit vaccines. BMC Bioinformatics. 2007; 8:1-7. [DOI:10.1186/1471-2105-8-4] [PMID]

[37] Haddad J, Whitehead G, Katsoulidis A, Rosseinsky M. In-MOFs based on amide functionalised flexible linkers. Faraday Discuss. 2017; 201:327-35. [DOI:10.1039/C7FD00085E] [PMID]

[38] Argos P. An investigation of oligopeptides linking domains in protein tertiary structures and possible candidates for general gene fusion. J Mol Biol. 1990; 211(4):943-58. [DOI:10.1016/0022-2836(90)90085-Z] [PMID]

[39] Arai R, Ueda H, Kitayama A, Kamiya N, Nagamune T. Design of the linkers which effectively separate domains of a bifunctional fusion protein. Protein Engin. 2001; 14(8):529-32. [DOI:10.1093/protein/14.8.529] [PMID]

[40] Chen X, Zaro JL, Shen WC. Fusion protein linkers: property, design and functionality. Adv Drug Delivery Rev. 2013; 65(10):1357-69. [DOI:10.1016/j.addr.2012.09.039] [PMID]

[41] Gokhale RS, Khosla C. Role of linkers in communication between protein modules. Curr Opin Chem Biol. 2000; 4(1):22-7. [DOI:10.1016/S1367-5931(99)00046-0] [PMID]

This Page Intentionally Left Blank